A Study on Interferential Tool Position Correcting Algorithm in Rough Machining of 3d Impeller Variable-axis Plunge Milling

Lei Dong (dongleishdj@126.com)
Shanghai DianJi university, 300 Shui Hua Rd., Shanghai 201306, People's Republic of China
Jie Wang
Shanghai Ocean University, 999 City Ring Rd., Shanghai 201306, People's Republic of China

Research Article

Keywords: 3D impeller variable-axis plunge milling, optimizing the cutter-axis vector, avoiding the interferential phenomenon, simulation verification

Posted Date: February 13th, 2021

DOI: https://doi.org/10.21203/rs.3.rs-212204/v1

A study on interferential tool position correcting algorithm in rough machining of 3D impeller variable-axis plunge milling

Dong Lei, Shanghai DianJi university, 300 Shui Hua Rd., Shanghai 201306, People's Republic of China, Email: dongleishdj@126.com, Fax: +8602138226253, Tel: +8613918511632
Wang Jie, Shanghai Ocean University, 999 City Ring Rd., Shanghai 201306, People's Republic of China, Email: wang-j@shou.edu.cn, Fax:+8602161900806, Tel:+8613817387056

Abstract The plunge milling method has remarkably improved the rough machining efficiency of 3D impeller channel. However, in conventional cutter position planning for plunge milling, interference at the end of every cutter position due to sudden increase of radial depth is inevitable, which may seriously compromise the service life of machine tool and cutter, as well as the cutting efficiency at the interferential phase. This study optimized the cutter axis vector for the tool path of conventional rough machining of 3D impeller variable -axis plunge milling to make the angle between the normal vector for workpiece surface at the cutter contact point and the cutter-axis vector of adjacent tool position increase gradually from outlet to inlet at the smallest scale. Based on this, an iterative algorithm for tool center position and safety height for the cutter was provided, thus making the hub allowance of the optimized tool path for plunge milling as small as possible without affecting the subsequent machining on the premise of avoiding the interferential phenomenon. Finally, the correctness of the proposed method was verified by relevant numerical examples.

Keywords 3D impeller variable-axis plunge milling · optimizing the cutter-axis vector · avoiding the interferential phenomenon · simulation verification

Declaration

Funding: Natural Science Foundation of Shanghai (Award Number:15ZR1417200)
Conflicts of interest: We declare that we do not have any commercial or associative interest that represents a conflict of interest in connection with the work submitted.
Availability of data and material: Not applicable
Code availability: Not applicable
Authors' contributions: Improve processing efficiency and machining precision of centrifugal 3D impeller
Ethics approval: Not applicable
Consent to participate: Yes
Consent for publication: Yes

1 Introduction

Centrifugal compressor is an important product in the equipment manufacturing industry, which is broadly applied in fields like metallurgy, petrochemistry, natural gas transportation, and air separation. The centrifugal 3D impeller is the core component of centrifugal compressor, and many scholars have attached much importance to its processing efficiency and manufacturing accuracy. For the 3D impeller, about 70-80% of material needs to be removed at the rough machining stage [1], indicating that improving the processing efficiency of the impeller should start with rough machining. With the development of relevant techniques, in the rough machining method for 3D impeller, the traditional five-axis side milling [2-6] has gradually been replaced by the high-speed milling [7], which has greatly improved the machining efficiency. However, the demand of impeller manufacturers still cannot be satisfied. In the plunge milling method, the tool is mainly subjected to axial force, while its rigidity in the axial direction is far better than that in the radial direction. Compared with end milling and side milling methods, the plunge milling method has a more stable process system. In view of its advantages in principle, the plunge milling method has attracted extensive attention worldwide in recent years, and its application starts from the blisk machining. In reference[1], Ren applied four-axis plunge milling method to the open blisk rough milling firstly in 2009. Dong[8] has done some research on the simulation of open blisk's four-axis plunging, and proposed a method of evaluating the residual and overcut of the material. Whether it is blisk or centrifugal 3D impeller, the cutting parameter and cutting mode of plunge milling are the key for improving the machining efficiency. Sun[9] proposed a new plunge milling tool path generation method using medial axis transform which could be used to control the radial depth to improve the cutting efficiency and cutter life. As for the cutting mode, in conventional plunge milling, the tool axes of every tool positions are parallel to each other. This mode is called as fixed axis milling [10], and also known as 3+2 axis plunge milling. Before processing, the angle of the two rotation axes for the five-axis machine tool is determined and locked, and during processing, only three straight axes are involved in the cutting process. If the tool axes of every tool positions are not parallel to each other, the mode is called as variable axis plunge milling [11]. Han[12] has done some research on plunge cutter selection and tool path generation algorithm, and applied it to the variable axis plunge milling of free-form surface impeller channel. In addition, sometimes the tool axis may change continuously during the plunge milling. For this, see Reference [13]. This method may also be classified as five-axis end milling, which is generally called as continuous variable axis milling. For the rough plunge milling of 3D impeller, no matter how the slotting way is performed, the interferential phenomenon is inevitable, and this phenomenon may seriously compromise the service life of both machine tool and cutting tool. Sun[14] is one of the few to present the phenomenon that the increase of radial depth often happens at the end of plunging phase and its influence on the service life of machine tool and the cutter, which is consistent with the suggestion proposed in this paper. Sun also proposed a solution method which is based on the thought to decrease the plunge depth to avoid the increase of radial depth

at the end of plunging phase. However, it is suitable for the plunge milling of axial flow blade and it is not suitable for the plunge milling of centrifugal impeller because it would leave large machining allowance on the hub surface which would bring great difficult to the subsequent hub finish machining. In addition to this, there is no any other documentation concerning this problem.

2 The interferential phenomenon during the rough plunge milling of 3D impeller

The interferential phenomenon refers to a difficulty in tool feeding during the plunge milling process resulting from the part without cutting blade at the bottom of flat-bottomed cutter involved in material cutting. See Fig. 1. In industrial production, the variable axis milling is the most commonly used for the rough milling of 3D impeller, and the reasons for this are as follows. First, the cutting efficiency of this method is high. Second, there are many automatic programming software products containing the variable axis plunge milling module, e.g., NREC, special for impeller machining, UG, a general CAD/CAM software, Powermill, Hypermill, and etc. However, no matter what kind of software is used for programming, the interferential tool position cannot be avoided. See Fig. 2. The reason for this is that in the plunge milling process, due to the distortion of the impeller hub surface, even if the planned radial cutting width is less than the cutting blade length at the bottom of the tool, there will be a part without cutting blade involved in cutting the residual layer of hub left by the previous tool position when the bottom part of flat-bottomed cutter is close to the hub surface. See Fig. 3. Thus, the interferential phenomenon occurs. Even if all cutting blades pass through the bottom surface center of cutter, due to the zero cutting speed at the center, the interferential phenomenon may still occur, resulting in a cutting difficulty accompanied by increasing cutting noise and tool vibration.

Undoubtedly, the most direct method for avoiding the interferential phenomenon is to adjust the cutter-axis vector, so that the tool may be tilted in the direction of the material to be cut as shown in Fig. 4. The angle for adjustment is very important. If the tilt angle is too small, the residual layer of hub left by the previous tool position cannot be avoided, and if the tilt angle is too large, the residual layer of hub will be excessively large, which may affect the overall planning for tool position and subsequent finish machining of hub surface.

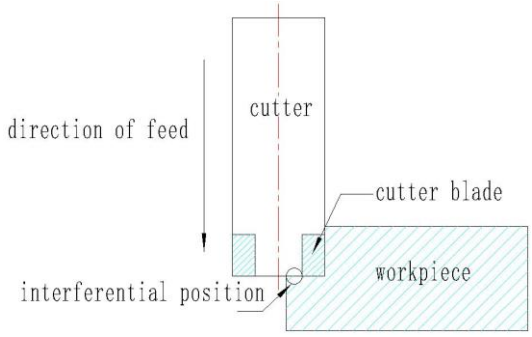

Fig. 1 Schematic diagram of interferential phenomenon

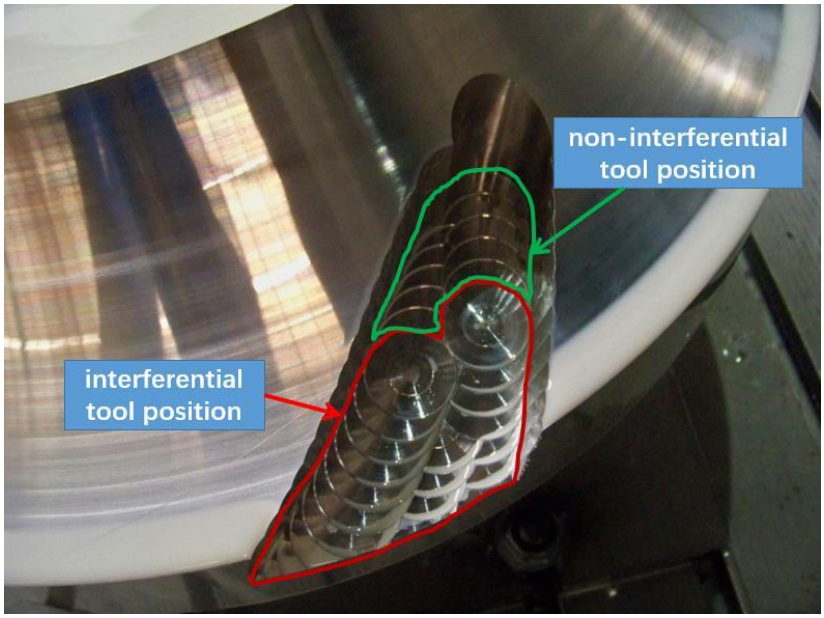

Fig. 2 Interferential tool position and non- interferential tool position

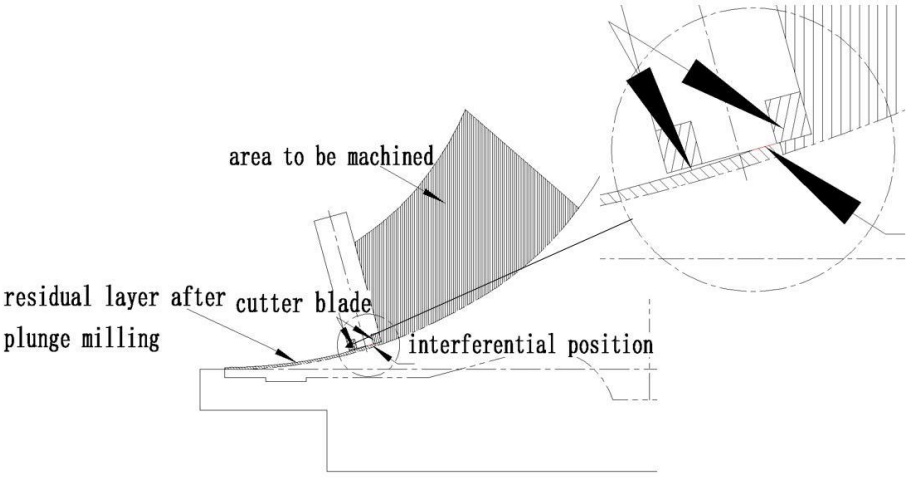

Fig. 3 Schematic diagram of interferential phenomenon for impeller plunge milling

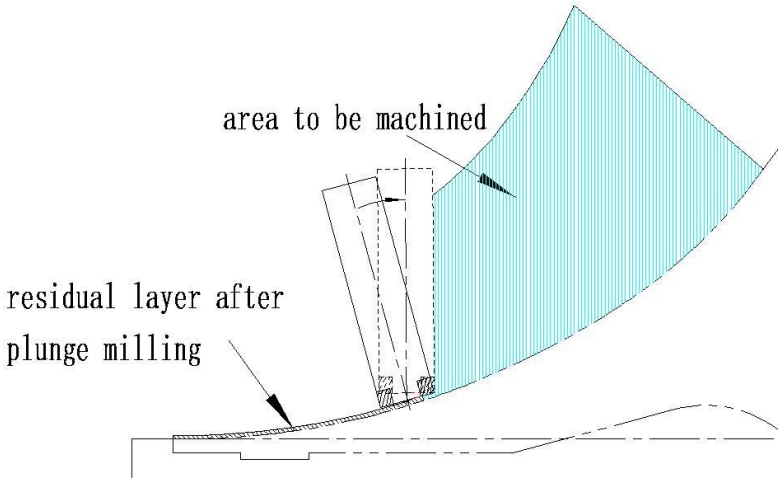

Fig. 4 Schematic diagram of the tilted direction of the cutter-axis vector

3 Tool axis vector optimization method

Based on the above analysis, the optimization may be summarized as follows. Make the angle between the normal vector for workpiece surface at the cutter contact point and the cutter-axis vector of adjacent tool position increase gradually from outlet to inlet at the smallest scale. The specific method is as follows:

① The cutter center point for the tool position in centrifugation 3D impeller variable axis rough plunge milling and the corresponding data points of shroud surface worked out by isoparametric method are extracted as shown in Fig. 5. Only a set of tool positions close to the suction surface of the blade is listed in the figure. Two NURBS curves are fitted by cutter center points Mi (i== 1, 2, 3,...,n) and the corresponding data points of shroud surface Wi (i=1,2,3,…,n) respectively as shown in Fig. 6.

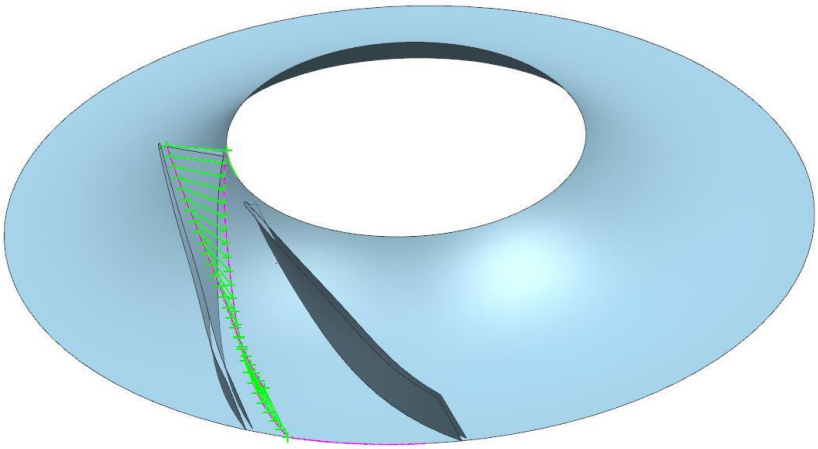

Fig. 5 A series of cutter center points and the corresponding data points of shroud surface extracted

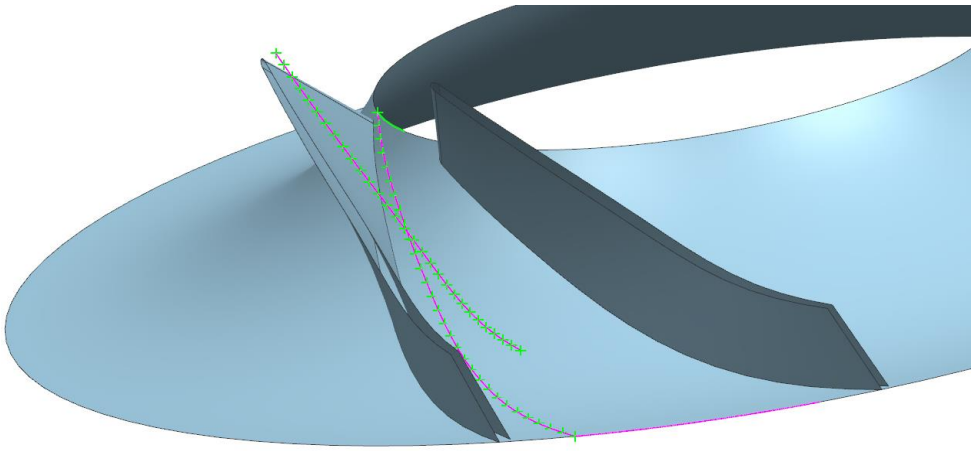

Fig. 6 Fitted NURBS curve

② Perform discrete processing for the NURBS curve. The smaller the walking distance, the smaller the cutter-axis vector adjusting angle to avoid the interferential

phenomenon. According to relevant experience, it is advisable to set the walking distance as 10-5 to obtain several discrete points, as shown in Fig. 7.

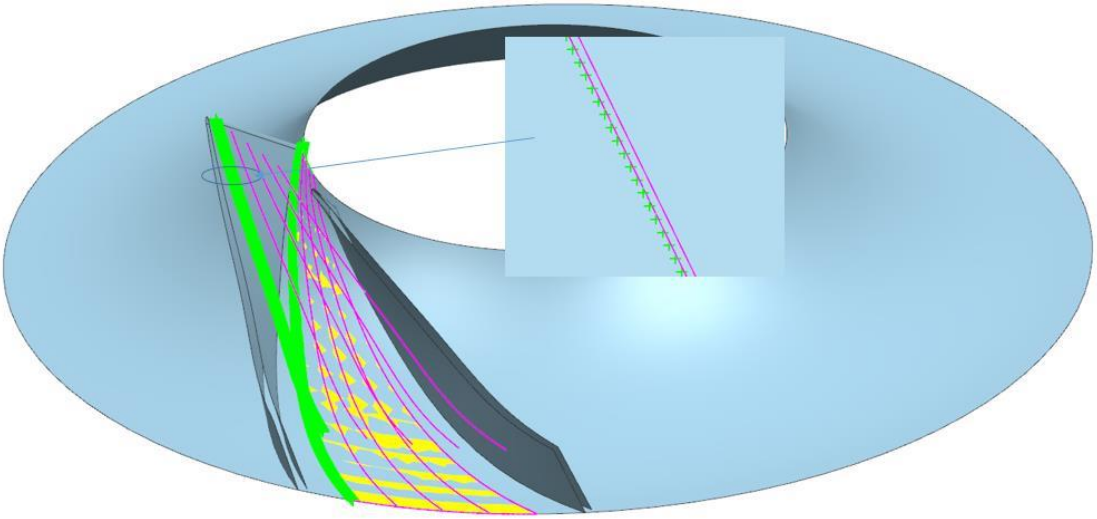

Fig. 7 Several discrete points obtained through discrete processing of NURBS curve

③ Establish the cutter axis vector optimization model as shown in Fig. 8. The feeding direction is from the outlet to the inlet. The tool position of variable axis plunge milling for each impeller channel is let to be m set. Take the tool position set of variable axis plunge milling near the suction surface of the impeller for instance, make a assumption that there are f tool position in this set. Then set the angle between the normal vector for the workpiece surface at the cutter contact point and the cutter axis vector as α_i (i=1,2,3,…,f) as shown in Fig. 9 (a), and set the intersection point of the cutter axis and the corresponding isoparametric line in shroud surface as W_i(i = 1, 2, 3,..., f) as shown in Fig. 9 (b). After the optimization starts, the first tool position remains unchanged, calculating α_2 and $\alpha 1$ for a comparison. And if $\alpha_2>\alpha_1$ is not satisfied, starting from W_2, search the discrete point sequence successively to the inlet direction of the impeller until a discrete point satisfying $\alpha_2>\alpha_1$ is obtained, and this discrete point is updated as Point W_2, and so on. Update W_i (i = 1, 2, 3,...,f) point sequence, and after this, $\alpha_n>\alpha_{n-1}\ldots\ldots\alpha_2>\alpha_1$. According to the cutter center point sequence M_i(i = 1, 2, 3,...f), intersection point sequence of cutter axis and the corresponding isoparametric line in shroud surface W_i (i= 1, 2, 3,...f), a new tool position sequence can be obtained through one-to-one calculation, and the interferential phenomenon will not occur in this set of tool positions, and so on, until all sets of tool positions are calculated.

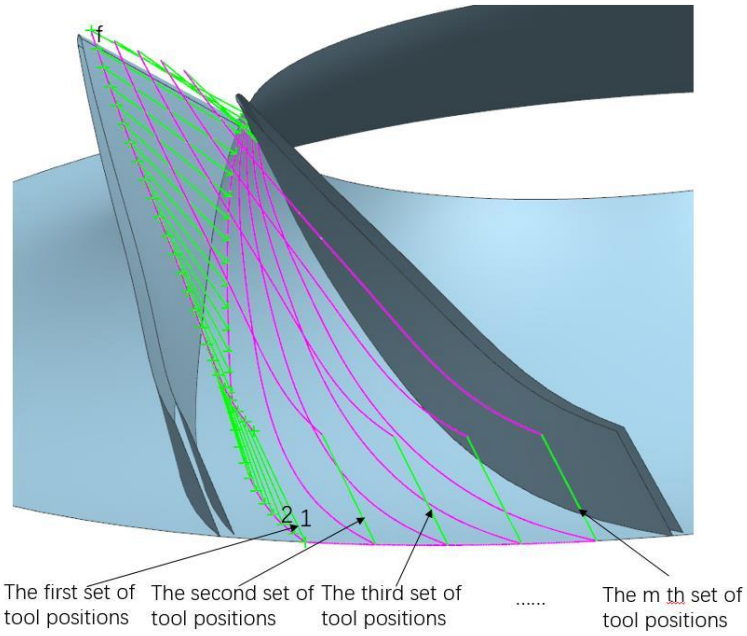

Fig. 8 Cutter positions sequence

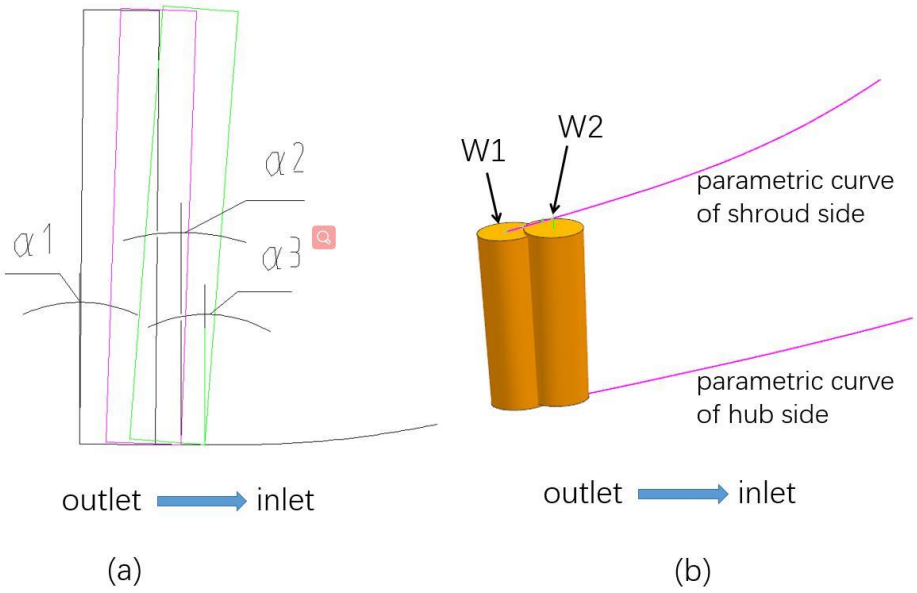

Fig. 9 Schematic diagram of cutter axis vector optimization

4 Determination of the slotting depth and the safety height for cutter

The optimized tool positions cannot guarantee the non-interferential contact between the cutter bottom and the hub surface anymore, and the cutter safety heights also needs to be recalculated. When processing impeller channel, not only the blade surface must be processed, but also the constraint of impeller hub surface must be considered, and so, the axial position of the tool also needs to be determined during plunge milling. The hub surface of impeller S_h is a rotative surface, which is

obtained through the curve on the hub surface c_p^h (intersection line of pressure surface and hub surface) or c_s^h （intersection line of suction surface and hub surface） turning around the rotary axis Z. The vector equation is as follows:

$$S_h:\ \mathbf{S}_h = \mathbf{S}_h(u,v) = \mathbf{B}(v)\mathbf{C}(u) \tag{1}$$

where $B(v) = \begin{bmatrix} \cos v & -\sin v & 0 \\ \sin v & \cos v & 0 \\ 0 & 0 & 1 \end{bmatrix}$ is the rotary set around the rotary axis Z, and v is the rotation angle rotating around the axis Z; $\mathbf{C}(u)$ is set as the vector representation of curve c_p^h, and u is the parameter.

As determining the axial position of plunge milling cutter, make the milling cutter move along the optimized direction of the cutter axis until the bottom plane of the milling cutter is in contact with the hub surface or the shroud surface without interference. If the hub surface and shroud surface are arbitrary free surfaces, the bottom plane of the milling cutter can be discretized for determining the axial position of the cutter. See Fig. 10 (b), after the projection point qi of each discrete point pi on the hub surface along the direction of the cutter axis is worked out, the axial position of the cutter can be determined with the minimum distance between corresponding points such as p7q7 as shown in Fig. 10 (a).

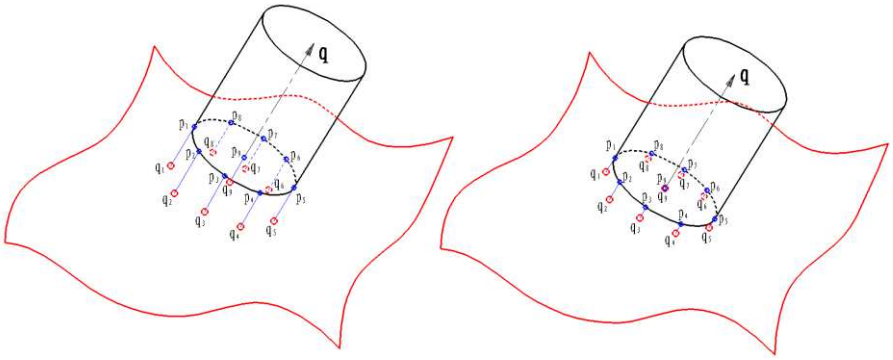

(a) （b）

Fig. 10 Determination of cutter's axial position in plunge milling of arbitrary free-form surface

Considering that the hub surface and shroud surface of the impeller are a rotative surface composed of hyperbolic points, it is relatively time-consuming to calculate the projection points of multiple discrete points on the bottom plane of the milling cutter on the surface to be processed. If the projection of the cutter bottom plane on the hub surface does not exceed the boundary of the hub surface, the interference-free contact point between the cutter bottom plane and the hub surface or the shroud surface must occur on the maximum excircle of the cutter bottom plane, based on which the axial position of cutter can be determined more efficiently. Here is a counter example to

prove the correctness of this conclusion. It is assumed that the interference free contact point between the bottom surface of the milling cutter and the hub surface occurs at point p1 within the maximum excircle, as shown in Fig. 11(a). Make two normal sections along the main direction of the impeller hub surface over point p1 as shown in Figs. 11(b) and 11(c) respectively. Fig. 11(b) shows the interference free contact point p1 between the cutter bottom plane and the hub surface is within the maximum excircle; Since both the hub surface and the shroud surface are composed of hyperbolic points, the bottom plane must interfere with the hub surface or the shroud surface as shown in Fig. 11(c). Therefore, the hypothesis is not true. That is, the interference free contact point between the bottom plane of the milling cutter and the hub surface or the shroud surface must occur on the maximum excircle of the bottom plane of the cutter.

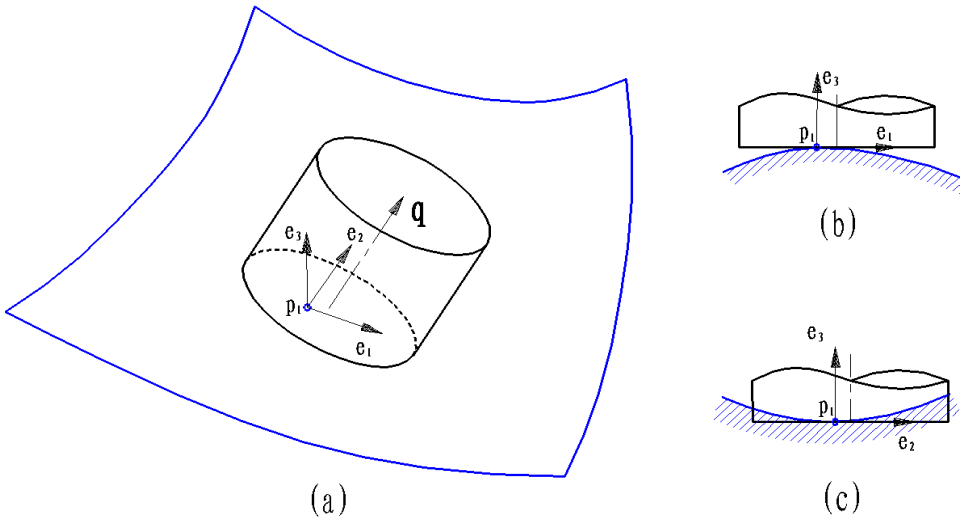

Fig. 11 Interference-free CC point between flat end of plunge milling cutter and hyperboloid

To determine the interference free contact point between the bottom plane of the cutter and the hub surface: Considering that the contact point occurs on the maximum excircle c on the bottom surface of the cutter, it is necessary to ensure that the bottom circle c and the hub surface not only contact at the cutter contact point, but also be tangent, so as to guarantee that there is no local interference between the bottom surface of tool and the hub surface at the cutter contact point. As shown in Fig. 12, the cutter contact point Q exists in the following two formulas:

$$\mathbf{P}+t\cdot\mathbf{q}+R\cdot\mathbf{r}=\mathbf{S}_h(u,v) \qquad (2)$$

$$\mathbf{T}\cdot\mathbf{n}=0 \qquad (3)$$

where $\mathbf{P}$ is a given point on the cutter axis, $\mathbf{q}$ is the axial unit vector of the cutter, i.e. the optimized cutter axis vector mentioned above; t is the displacement parameter of point $\mathbf{P}$ along the vector $\mathbf{q}$; R is the radius of the cutter, r is any radial unit vector for bottom plane of the flat bottom cutter; $\mathbf{T}$, the unit vector on the

bottom plane of flat bottom cutter and perpendicular to the vector r, and n, the unit normal vector at the contact point Q on the hub surface.

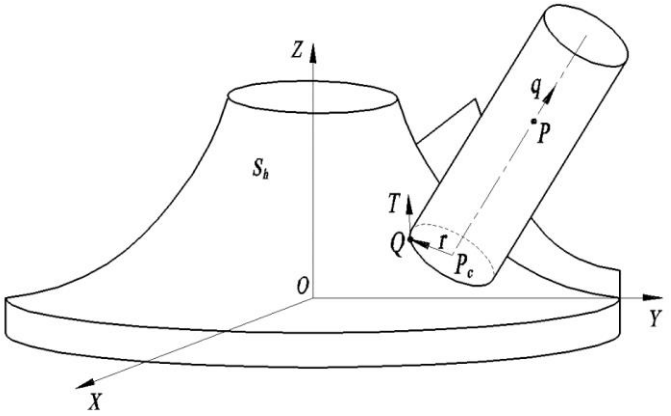

Fig. 12 Determination of axial position of cutter in plunge milling hub surface

On account of the vector T is perpendicular to the vector q and n at the same time, therefore

$$\mathbf{T}=\frac{\mathbf{q}\times\mathbf{n}}{\|\mathbf{q}\times\mathbf{n}\|} \tag{4}$$

$$\mathbf{r}=\mathbf{q}\times\mathbf{T} \tag{5}$$

Formula (4) is invalid if $\mathbf{q}$ and $\mathbf{n}$ are parallel to each other. At this point, set T as follows:

$$\mathbf{T}=\frac{\mathbf{q}\times\mathbf{PQ}}{\|\mathbf{q}\times\mathbf{PQ}\|} \tag{6}$$

Where $\mathbf{PQ}$ is the vector quantity of the cutter contact point $\mathbf{Q}$ pointing to a given point $\mathbf{P}$ on the cutter axis. Substitute Formula (5) into Formula (2), and carry out Taylor expansion on Formula (2), omitting the infinitesimal above the first order, thus obtaining the following formula:

$$\mathbf{q}\cdot\Delta t-\mathbf{S}_{h\_u}\cdot\Delta u-\mathbf{S}_{h\_v}\cdot\Delta v=\mathbf{S}_h(u_0,v_0)-\mathbf{P}-R\cdot\mathbf{r} \tag{7}$$

where Δt, Δu and Δv are the first order infinitesimal of parameters t, u and v, u_0, v_0, surface parameters of the given initial point on the hub surface. And $\mathbf{S}_{h\_u}=B(v)\mathbf{C}_u(u)$, $\mathbf{S}_{h\_v}=B_v(v)\mathbf{C}(u)$, where $\mathbf{C}_u(u)$ is the first derivative of curve c_p^h, $B_v(v)=\begin{bmatrix}-\sin v & -\cos v & 0\\ \cos v & -\sin v & 0\\ 0 & 0 & 0\end{bmatrix}$ is the derivative of rotative set $B(v)$ with respect to v, set $\mathbf{V}=\mathbf{S}_h(u_0,v_0)-\mathbf{P}-R\cdot\mathbf{r}$, dot product two endpoints of Formula (7) respectively by $\mathbf{q}$、$\mathbf{S}_{h\_u}$、$\mathbf{S}_{h\_v}$, thus obtaining the following Formulas

$$\begin{bmatrix} \mathbf{q}\cdot\mathbf{q} & -\mathbf{S}_{h\_u}\cdot\mathbf{q} & -\mathbf{S}_{h\_v}\cdot\mathbf{q} \\ \mathbf{q}\cdot\mathbf{S}_{h\_u} & -\mathbf{S}_{h\_u}\cdot\mathbf{S}_{h\_u} & -\mathbf{S}_{h\_v}\cdot\mathbf{S}_{h\_u} \\ \mathbf{q}\cdot\mathbf{S}_{h\_v} & -\mathbf{S}_{h\_u}\cdot\mathbf{S}_{h\_v} & -\mathbf{S}_{h\_v}\cdot\mathbf{S}_{h\_v} \end{bmatrix} \cdot \begin{bmatrix} \Delta t \\ \Delta u \\ \Delta v \end{bmatrix} = \begin{bmatrix} \mathbf{V}\cdot\mathbf{q} \\ \mathbf{V}\cdot\mathbf{S}_{h\_u} \\ \mathbf{V}\cdot\mathbf{S}_{h\_v} \end{bmatrix} \quad (8)$$

Through solving the Formulas, $\Delta t, \Delta u, \Delta v$ are obtained, set: $t+\Delta t \to t$, $u+\Delta u \to u$, $v+\Delta v \to v$, repeat the above procedure until $|\Delta t| \le \varepsilon$, $|\Delta u| \le \varepsilon$, $|\Delta v| \le \varepsilon$ (ε , the iterative accuracy), and then, the tangent point between the circle c on the end face of the flat bottom plunge milling cutter and the hub surface can be obtained. At this point, the vector equation of the cutter center $\mathbf{P}_c$ is as follows:

$$\mathbf{P}_c = \mathbf{P} + t\cdot\mathbf{q} \quad (9)$$

The same method is used to calculate the point of tangency between the bottom plane of the tool and the shroud surface of impeller, and then the safe lifting height of cutter for plunge milling may be determined in combination with appropriate safety distance. If there is cutter tip fillet, just offset the hub surface along its normal direction to the tool tip fillet radius. The determination process for cutter axial position is similar to the above.

5 Numerical examples

A simulation example is given based on a centrifugal semi-open 3D impeller, with channel divided into three sections to make a rough machining of variable axis plunge milling. The cutting direction is from the outlet to the inlet. For the outlet section, use a Ø30 flat bottom plunge milling cutter, for the middle section, use a Ø16 one, and for the inlet section, use a Ø8 one. The simulation results before cutter axis vector optimization are as shown in Fig. 13. Obviously, the overall residual layer of hub surface presents a down-step trend, indicating that at each stage before the feed for plunge milling near the hub, the parts of the tool bottom other than the main cutting blade are in contact with the residual layer of hub surface left by the previous tool position, i.e., the interferential phenomenon occurs. The tool axis vector optimization was carried out for the three sections of plunge milling tool position respectively, and the slotting depth and safety height of tool were updated. When the tool, cutting parameters and cutting direction were unchanged, the simulation results after optimization were as shown in Fig. 14. Obviously, the overall residual layer of hub surface shows an up-step trend after optimization, and thus, every time the plunge milling feeds near the hub, the residual layer of hub surface left by the previous cutter location may be avoided, and the interferential phenomenon will not occur.

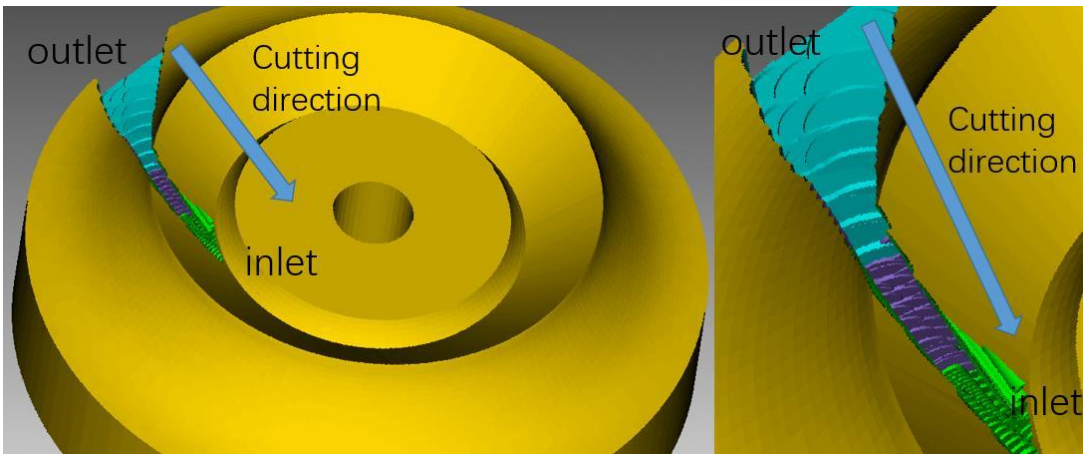

Fig. 13 Cutting simulation results before cutter axis vector optimization

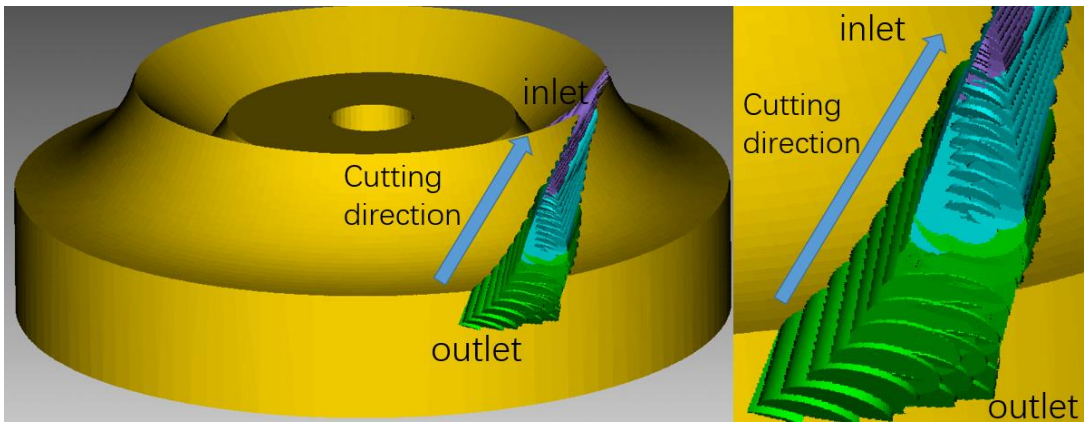

Fig. 14 Cutting simulation results after cutter axis vector optimization

6 Summary

In order to avoid the interferential phenomenon in the rough machining of variable axis plunge milling of 3D impeller, cutter axis vector optimization was performed for the tool position for variable axis plunge milling, in which the angle between the normal vector for workpiece surface at the cutter contact point and the cutter-axis vector of adjacent tool position was increased gradually from outlet to inlet at the smallest scale. Based on this, an iterative algorithm for tool center position and safety height for the cutter was provided, thus making the hub allowance of the optimized tool path for plunge milling as small as possible without affecting the subsequent machining on the premise of avoiding the interferential phenomenon. At last, the correctness of the proposed method was verified by relevant numerical examples.

Acknowledgments The research was supported by Natural Science Foundation of Shanghai (no. 15ZR1417200)

References

1. Ren JX, Yao CF, Zhang DH, Xue YL(2009) Research on tool path planning method

of four-axis high-efficiency slot plunge milling for open blisk[J]. Int J Adv Manuf Technol 45(1): 101–109
2. Young HT, Chuang LC, Gerschwiler K(2004)A five-axis rough machining approach for a centrifugal impeller. Int J Adv Manuf Technol 23(3-4):233–239
3. Lim P(2009) Optimization of the rough cutting factors of impeller with five-axis machine using response surface methodology. Int J Adv Manuf Technol 45(7-8):821-829
4. Fan HZ, Wang W, Xi G(2013) A novel five-axis rough machining method for efficient manufacturing of centrifugal impeller with free-form blades. Int J Adv Manuf Technol 68(5~8):1219–1229
5. Fan HZ.,Xi G.,Wang W.,Cao YL(2016) An efficient five-axis machining method of centrifugal impeller based on regional milling. Int J Adv Manuf Technol 87:789–799
6. Han FY,Zhang CW,Guo W,Peng XL,Zhang W(2018) A high-efficiency generation method of integral impeller channel tool path based on parametric domain template trajectory mapping. Int J Adv Manuf Technol 100:75–85
7. Pei LQ，Wei GJ，Bi HB. Study of linear axes milling method in 3D impeller(2013) Chinese Journal of Compressor Blower & Fan Technology 2:49-51
8. Dong JS,Chang ZY,Chang Y,Chen ZZ, Wang N(2019) A novel approach to modeling of multi-axis plunge milling and its application on the simulation of complex part plunging. Int J Adv Manuf Technol 102:1041–1051
9. Sun C,Wang YH,Huang ND(2015) A new plunge milling tool path generation method for radial depth control using medial axis transform. Int J Adv Manuf Technol 76: 1575–1582
10. Dong L,Cao LX(2014) Research on the approximating method of tunnel surface with general cylindrical surface and its application in the plunge milling of impeller. Chinese Journal of Acta Aeronautica et Astronautica 35(8):2331-2340
11. Li T，C WY，Chen CH(2010) Rough machining method for blisk plunge milling. Chinese Journal of Computer integrated manufacturing systems 16（8）：1696-1701
12. Han FY,Zhang DH,Luo M,Wu BH(2014) Optimal CNC plunge cutter selection and tool path generation for multi-axis roughing free-form surface impeller channel. Int J Adv Manuf Technol 71:1801–1810
13. Sun J,Cai YL(2009) Machining Simulation for Axial- Flow Hydraulic Turbine Blade. Chinese Journal of Equipment manufacturing technology（7）：5-7
14. Sun C,Bi QZ,Wang YH,Huang ND(2015) Improving cutter life and cutting efficiency of five-axis plunge milling by simulation and tool path regeneration. Int J Adv Manuf Technol 77: 965–972

Figures

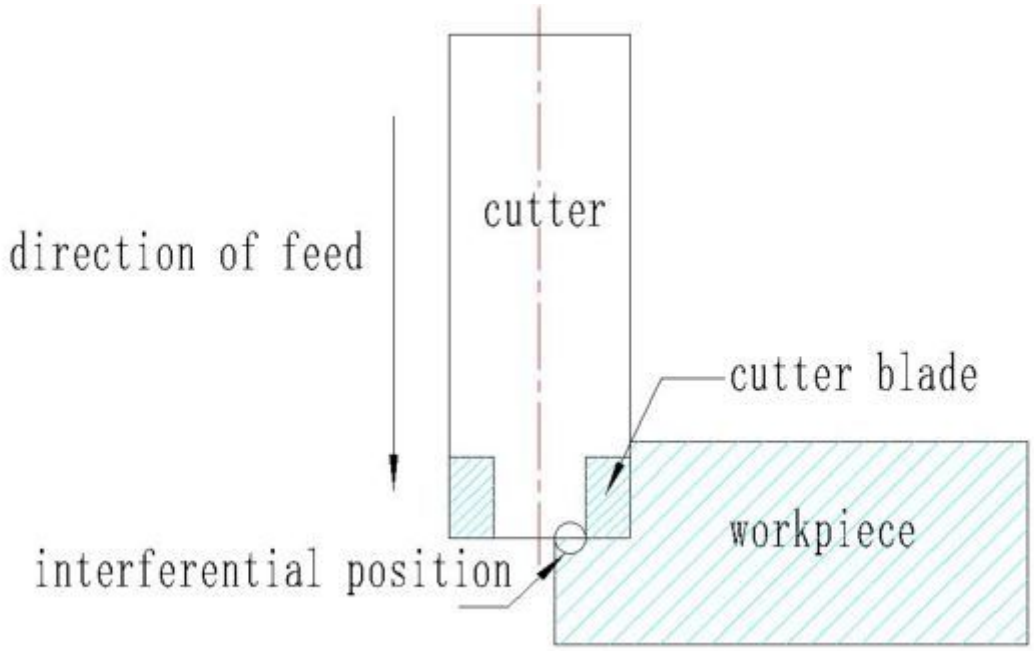

Figure 1

Schematic diagram of interferential phenomenon

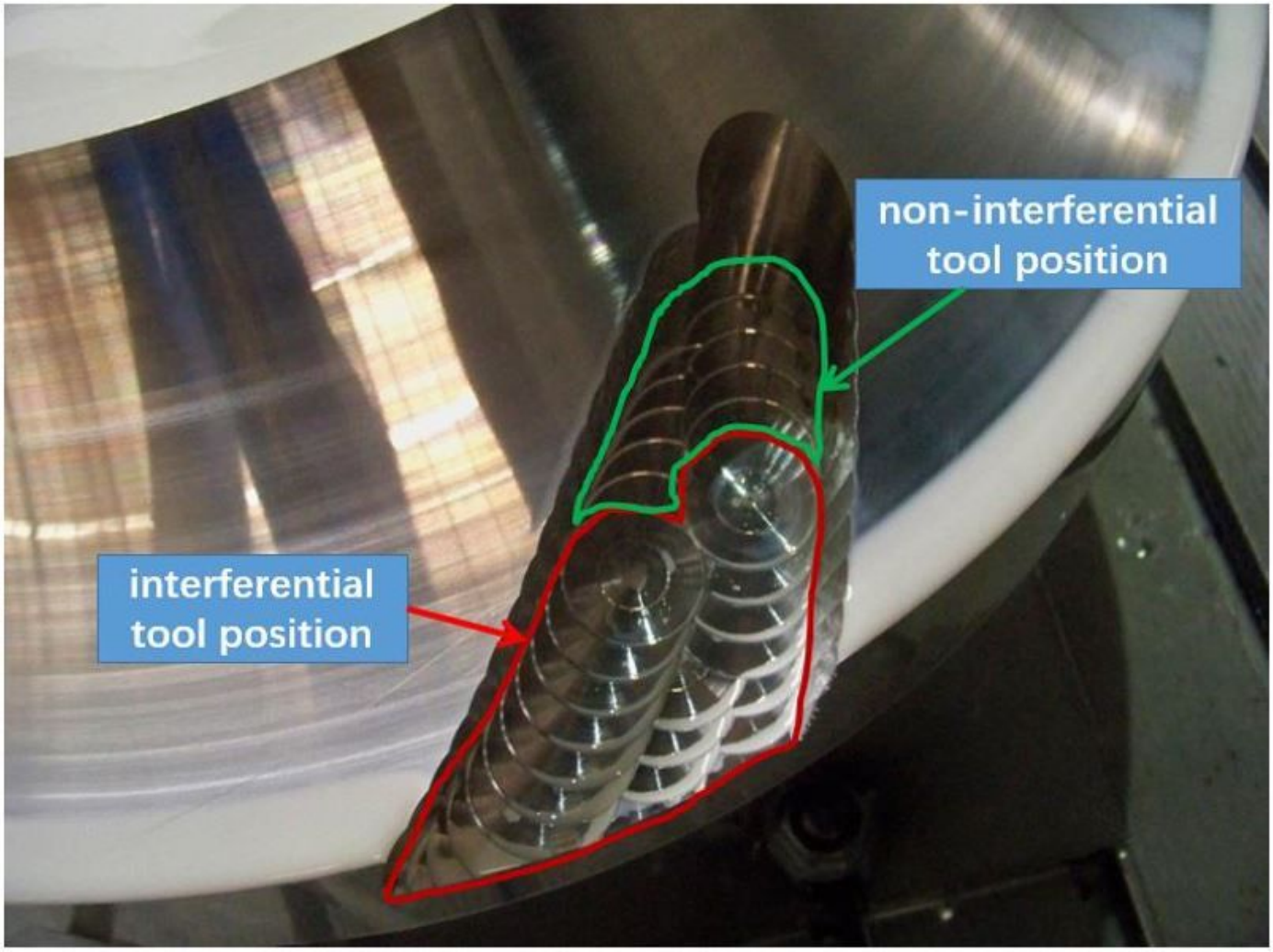

Figure 2

Interferential tool position and non- interferential tool position

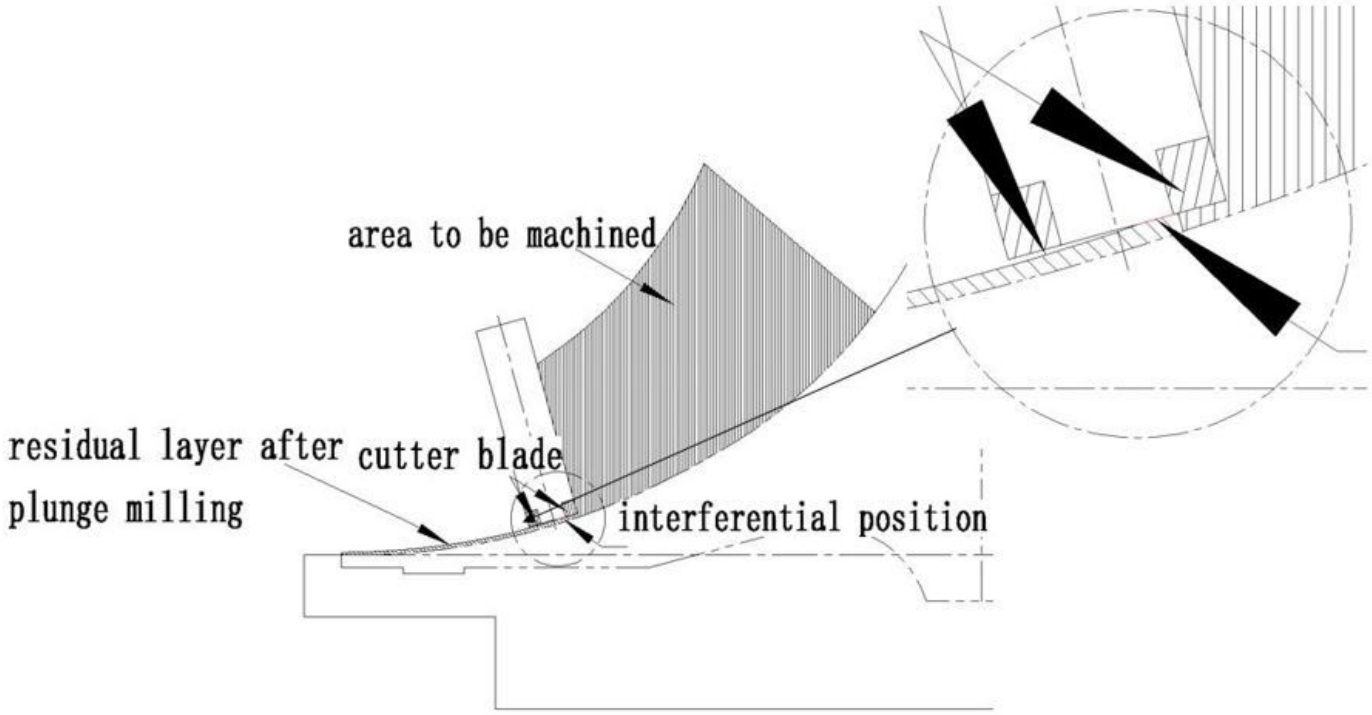

Figure 3

Schematic diagram of interferential phenomenon for impeller plunge milling

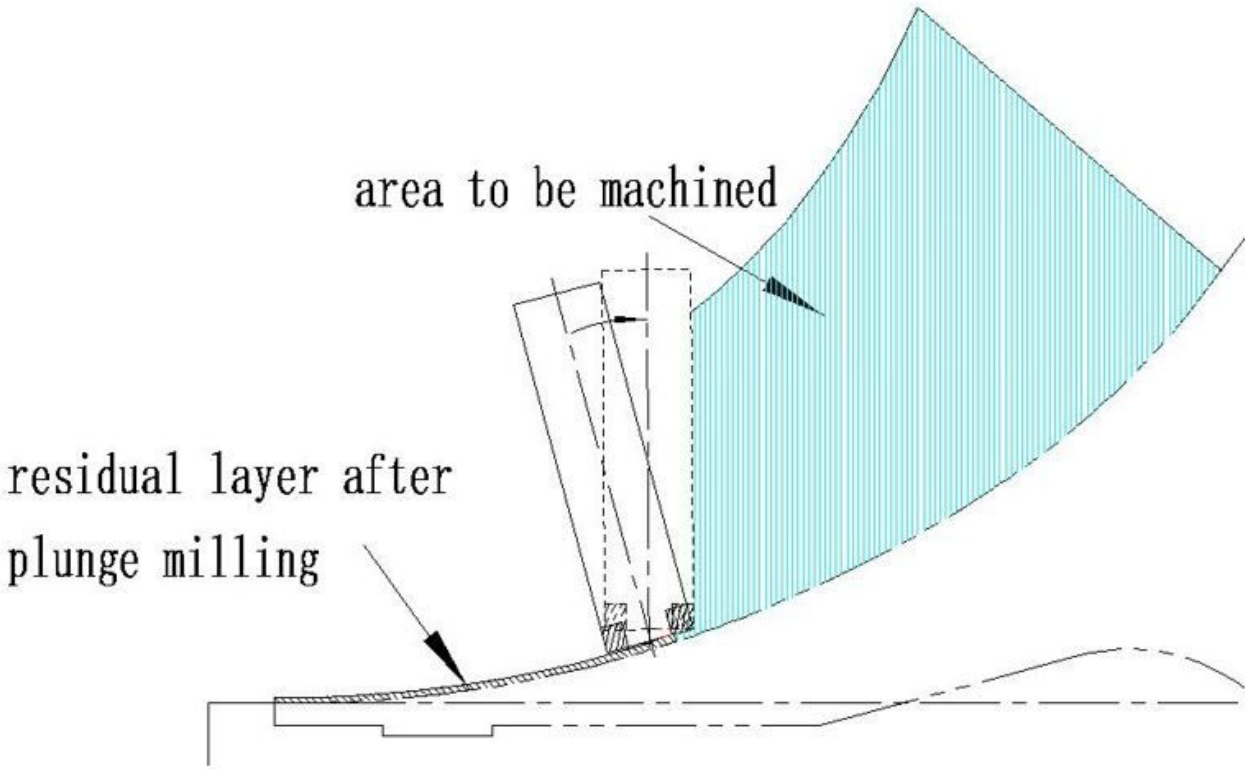

Figure 4

Schematic diagram of the tilted direction of the cutter-axis vector

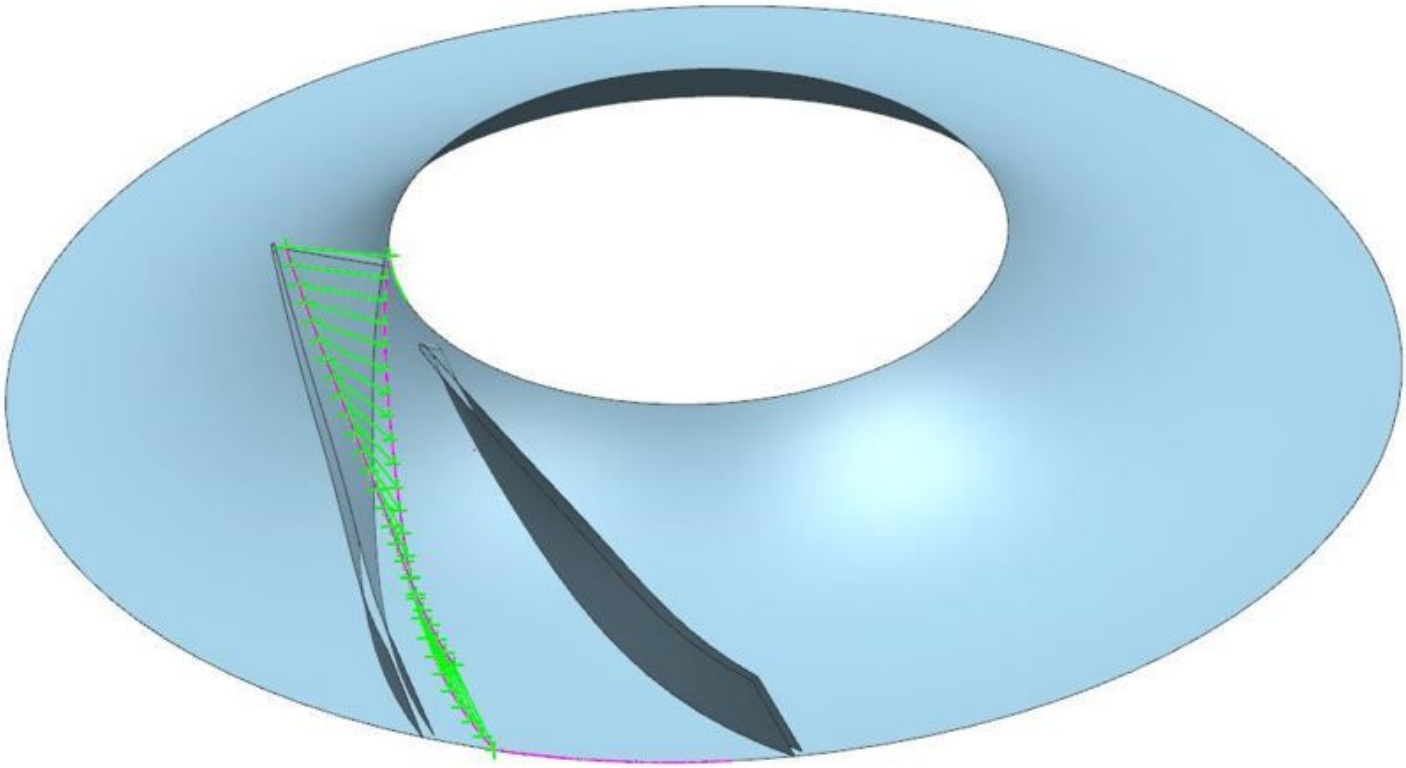

Figure 5

A series of cutter center points and the corresponding data points of shroud surface extracted

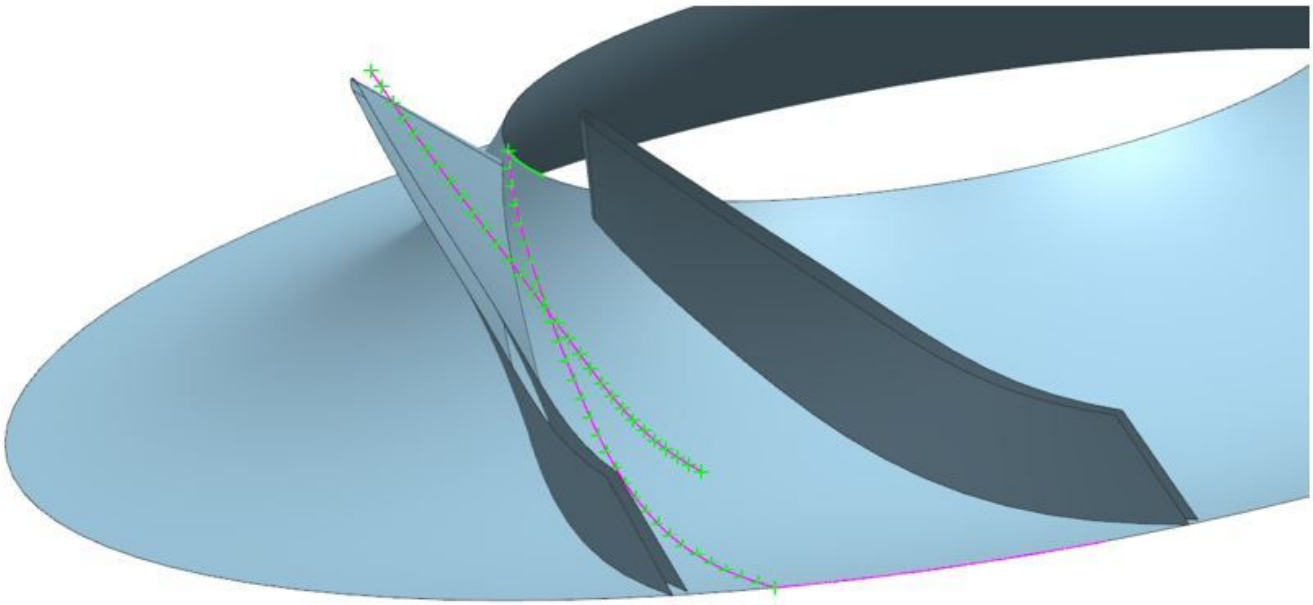

Figure 6

Fitted NURBS curve

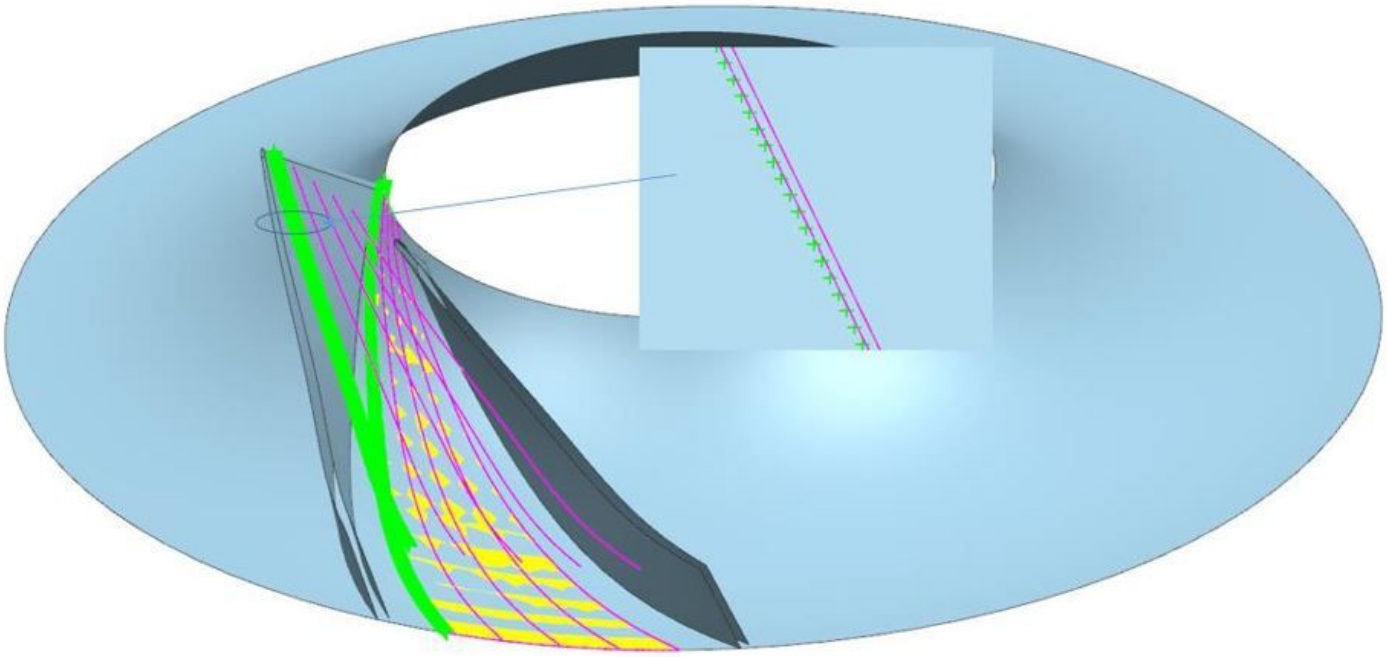

Figure 7

Several discrete points obtained through discrete processing of NURBS curve

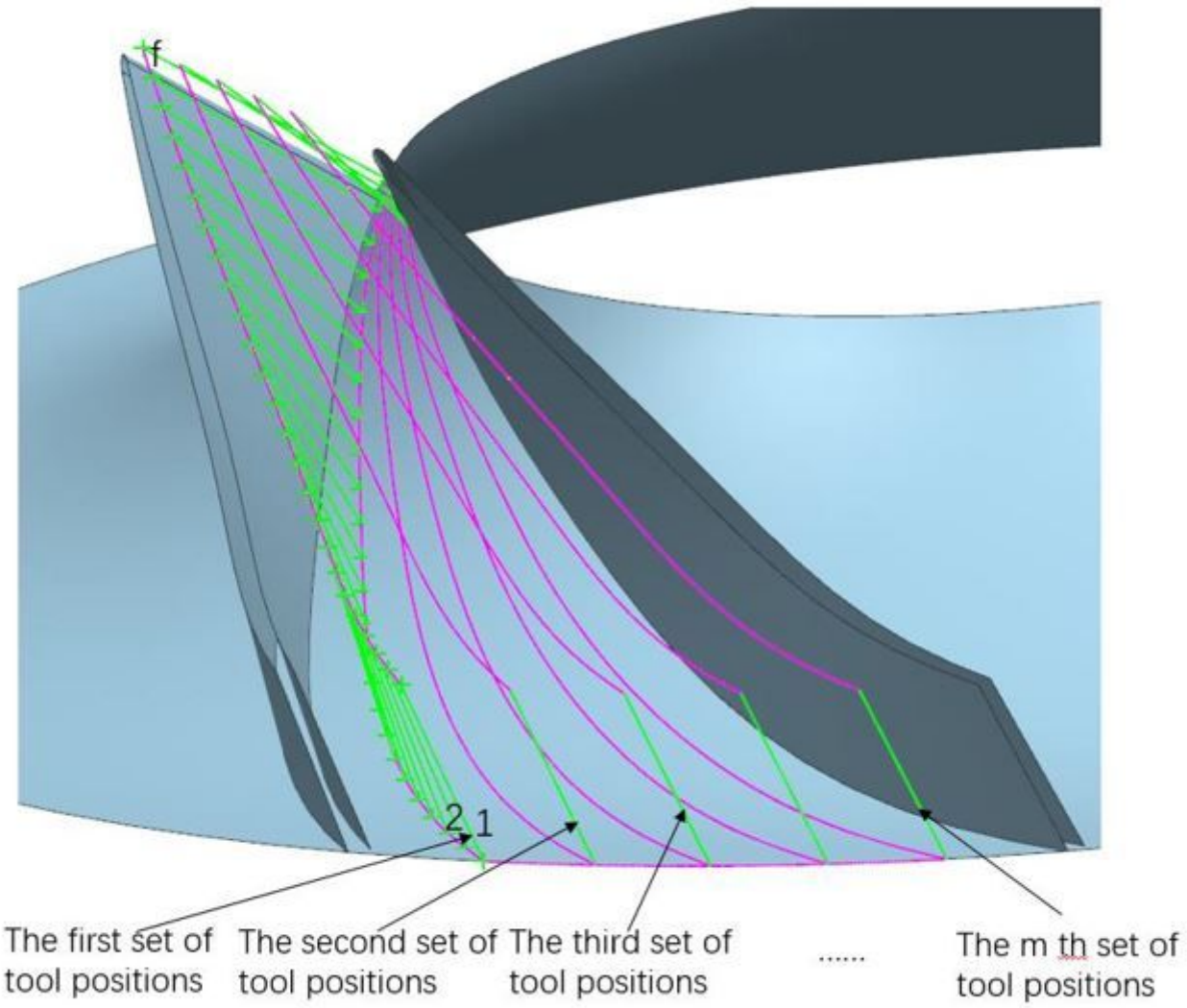

Figure 8

Cutter positions sequence

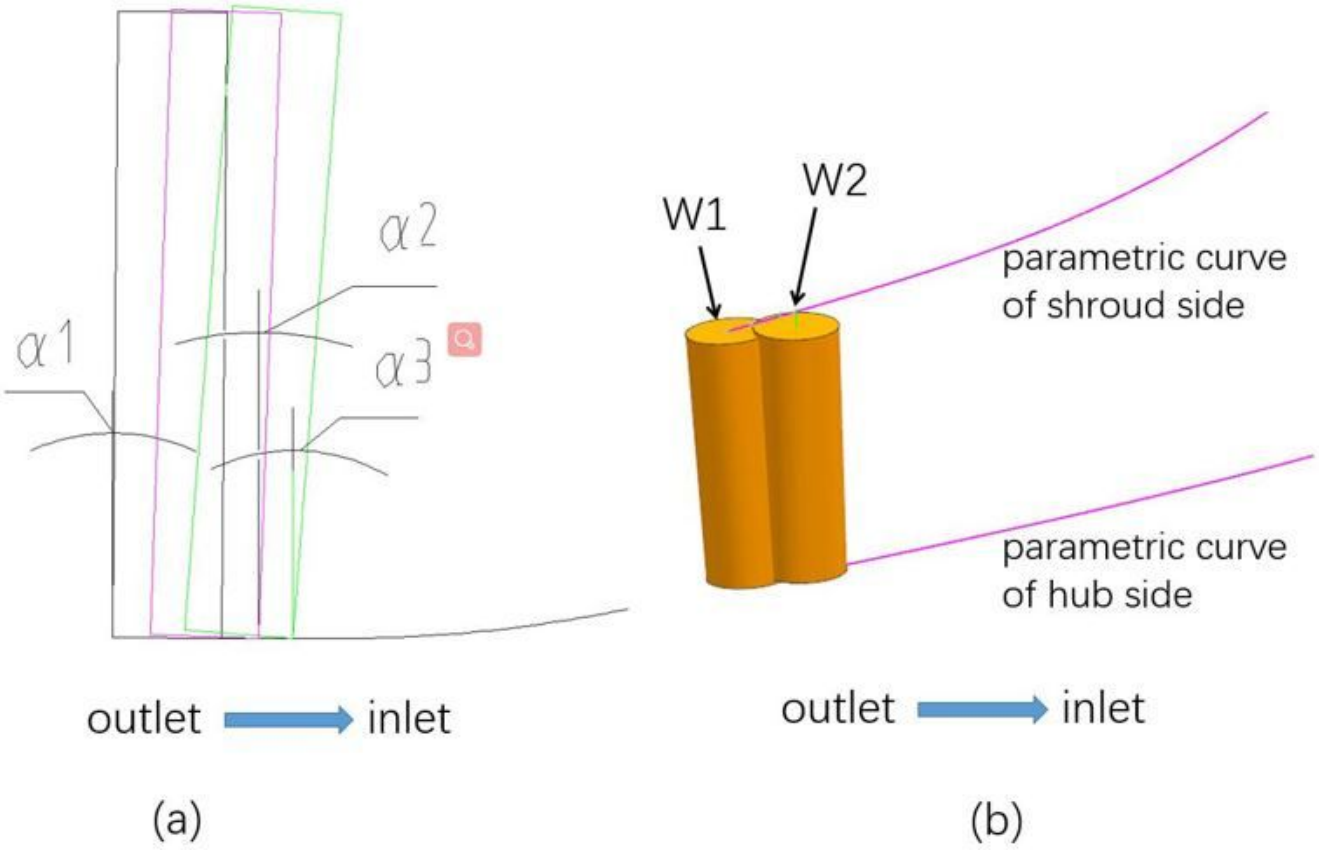

Figure 9

Schematic diagram of cutter axis vector optimization

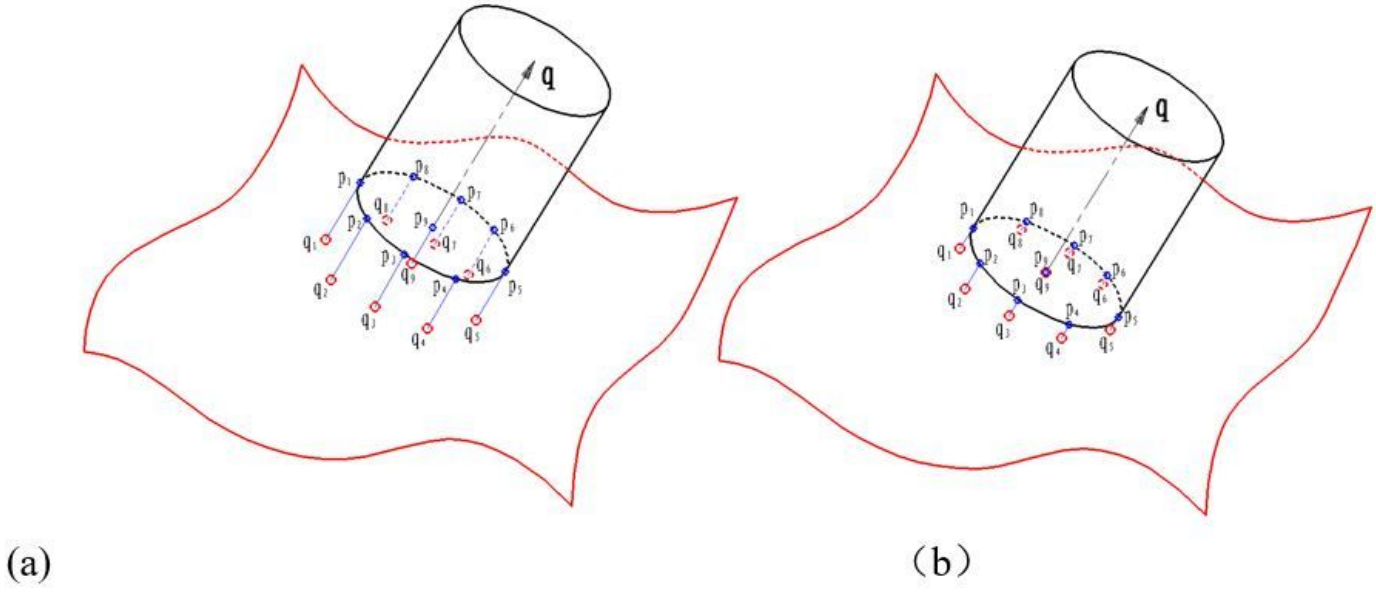

Figure 10

Determination of cutter's axial position in plunge milling of arbitrary free-form surface

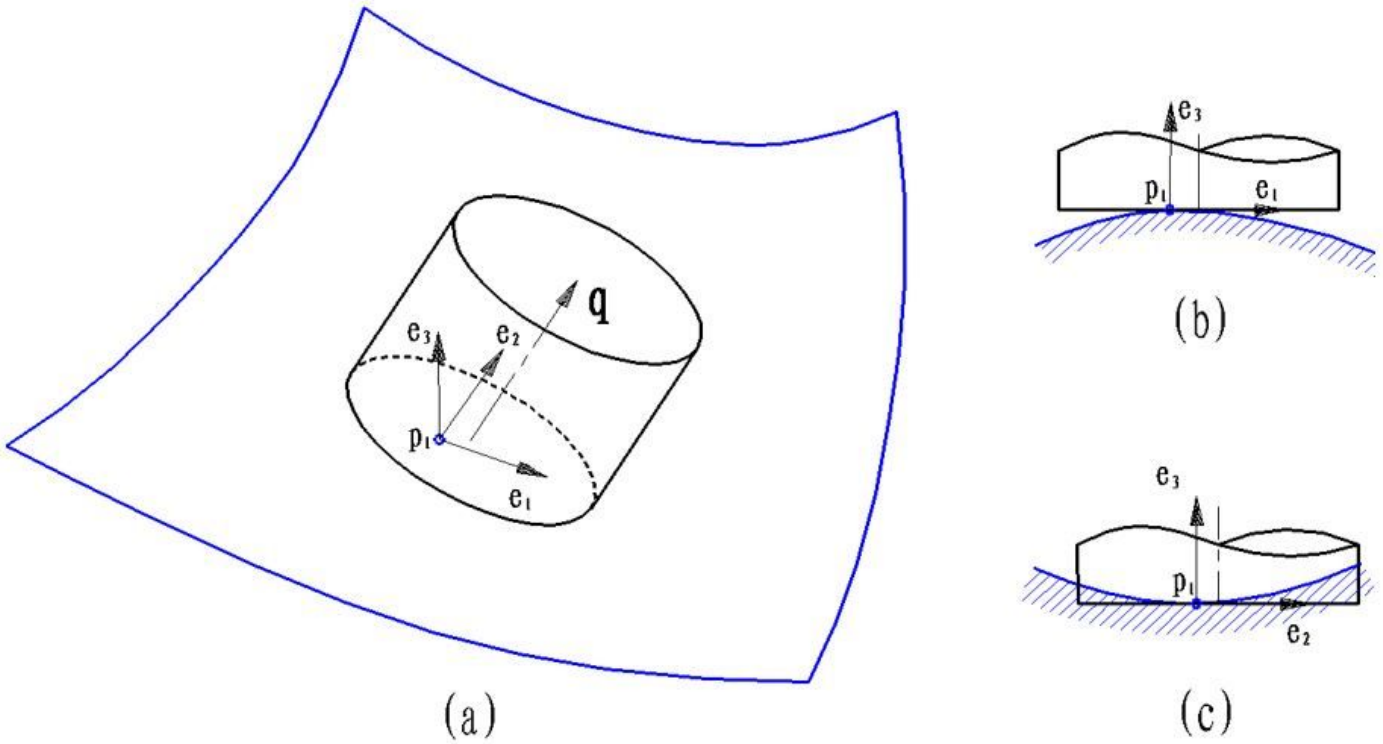

Figure 11

Interference-free CC point between flat end of plunge milling cutter and hyperboloid

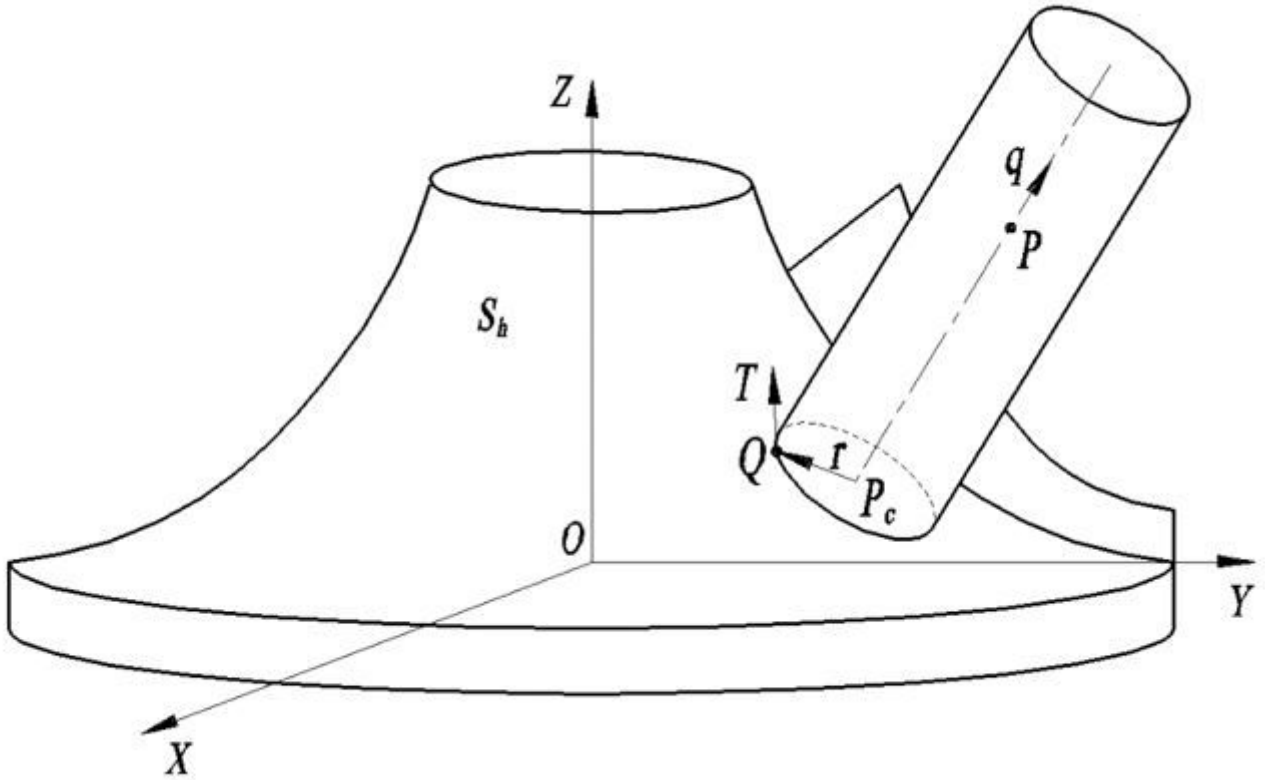

Figure 12

Determination of axial position of cutter in plunge milling hub surface

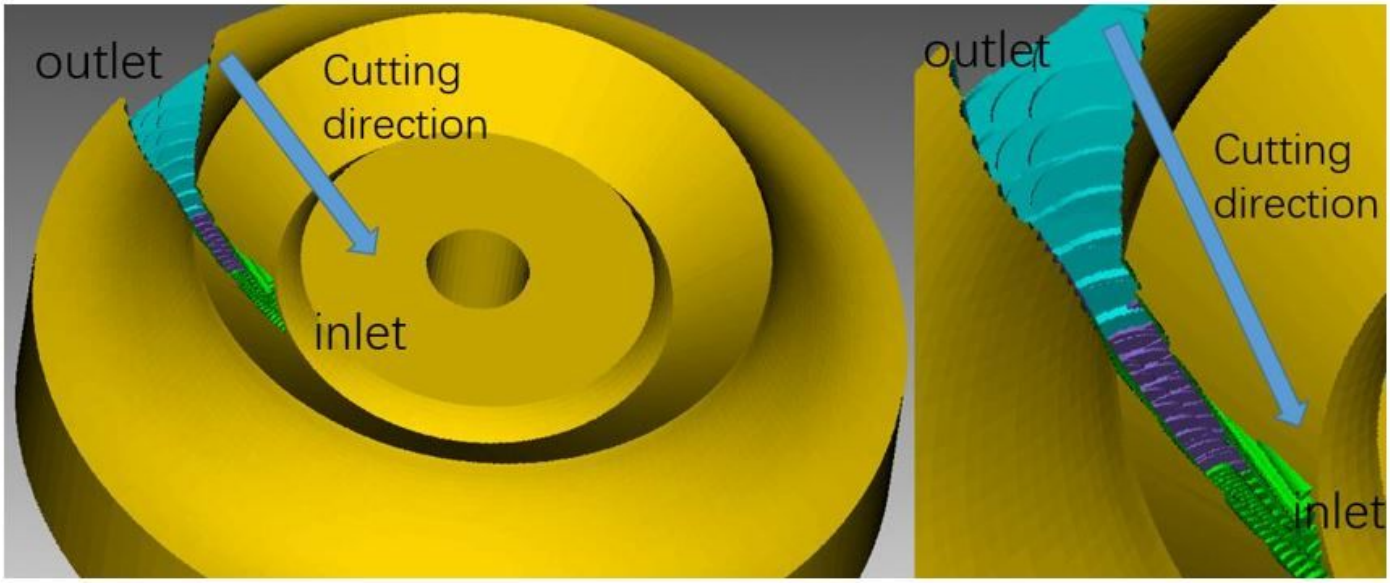

Figure 13

Cutting simulation results before cutter axis vector optimization

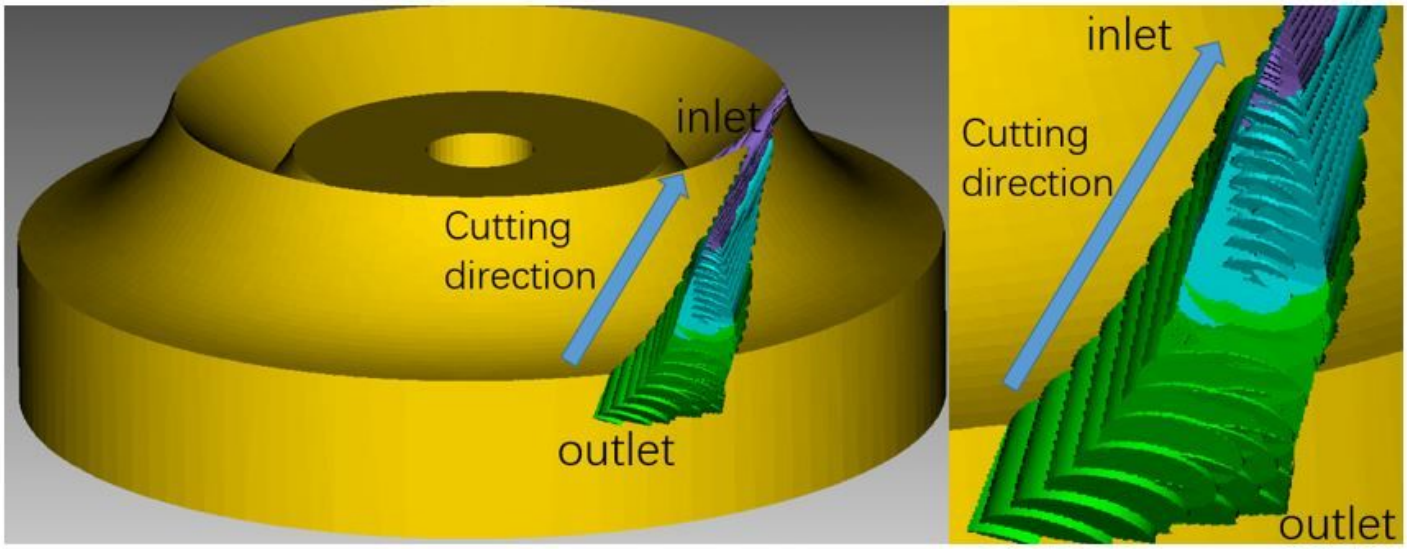

Figure 14

Cutting simulation results after cutter axis vector optimization